Bull. Inst. Chem. Res., Kyoto Univ., Vol. 70, No. 1, 1992

# Lifetime Control in Thyristors by Proton Irradiation

Hajime AKIYAMA, Hisao KONDOH, Katsumi SATOH*, Tsutomu NAKAGAWA*, Takashi FUJIMOTO**, Yoshihisa IWASHITA*** and Makoto INOUE***

*Received February 10, 1992*

The localized lifetime control effect by proton irradiation was studied for improving the performance of the large diameter high power semiconductor device. An extra beam transport system was connected to the Kyoto University 8UDH tandem pelletron in order to defocus the proton beam for large area irradiation. The experimental results show that this technology is useful to improve the characteristics of the 40mm$\phi$ silicon power diode and thyristor.

KEY WORDS: Semiconductor/ Power device/ Lifetime control/ Proton/ Diode/ Thyristor/

## INTRODUCTION

The turn-off switching speed of the power semiconductor device is enhanced by the lifetime reduction of the minority carrier in silicon. This lifetime in silicon depends on the density of the carrier recombination center, which is customarily introduced by the diffusion process of heavy metal, such as gold, into the device or by electron irradiation[1]. The diffusion process of gold leads to a relatively uniform distribution of the recombination center throughout the device. In case of the electron irradiation, the energy in excess of about 1 MeV is necessary to produce the defect which acts as the recombination center. At these energies, the range of electron is larger than the device thickness, and it causes a relatively uniform distribution of the defects. When light ion irradiation, such as protons or helium ions, is used, most of the defects are created around the end of the range of these ions. Then, we can achieve the localized lifetime control by choosing the appropriate energy of the ions.

Generally, the reduction of the lifetime enhances the turn-off switching speed of the power devices, but it increases the on-state voltage during conduction. Therefore, there is a trade-off relation between the turn-off time and the on-state voltage[2]. Recently, it was reported that the light ion irradiation resulted in more desirable trade-off relation than electron irradiation for the middle power devices such as IGBTs (Insulated Gate Bipolar Transis-

秋山 肇, 近藤久雄: LSI Lab., Mitsubishi Electric Corp., 4-1 Mizuhara, Itami City, Hyogo 664.
* 佐藤克己, 中川 勉: Fukuoka Works, Mitsubishi Electric Corp., 1-1-1 Imajukuhigashi, Nishiku, Fukuoka City, Fukuoka 819-01.
** 藤本 爵: Technical Research Center, The Kansai Electric Power Corp., Inc., 11-20 Nakoji 3-chome, Amagasaki, Hyogo 661.
*** 岩下芳久, 井上 信: Accelerator Lab., Nuclear Science Research Facility, Institute for Chemical Research, Kyoto University, Uji City, Kyoto 611.

tor)[3)4)5)]. There have been some reports about the lifetime control in the high power diode, thyristor and GTO by the proton irradiation[6)7)8)], in which, however, the improvement of the trade-off relation compared with the conventional technology has not been examined.

In the present experiment, the lifetime control by proton irradiation is studied for improving the trade-off relation between the turn-off time and the on-state voltage of high power thyristors and diodes.

## EXPERIMENTAL SETUP AND PROCEDURE

We adopted high power diodes (diameter: 40mm, thickness: 660$\mu$m) and high power thyristors (diameter: 40mm, thickness: 930$\mu$m) as the samples for studying the lifetime control by the proton irradiation. The proton irradiation was performed by the Kyoto University 8UDH trandem pelletron. This machine is able to accelerate protons up to the energy of 16MeV[9)]. Fig. 1 shows the relation between the proton range in silicon and the proton energy. The figure indicates that the lifetime at any desired depth in the sample device can be controlled by the proton having various energy less than 12MeV. We designed an extra beam transport system to obtain large irradiation field. It is already reported that a scanning magnet is useful for getting large area of the uniform irradiation field[10)]. We used a defocusing magnet system beside the use of a 60Hz scanning magnet to realize the large irradiation area. Calculation of the beam image, by "TRANSPORT" program[11)], showed that maximum area of uniform irradiation would be 100mm in diameter at the proton energy of 10 MeV by optimizing the magnet parameter.

A CsI scintillation plate and a CTA-film[12)13)] were used for checking the beam image, and the beam flux uniformity, respectively. The area of the defocused beam image was observed to be larger than the area of the sample devices. The proton dose, measured by integrating the beam current, was varied in the range from $10^{10}$ to $10^{12}$ p/cm$^2$.

After the irradiation, the depth profile of the spreading resistance ($R_{SR}$) in silicon which corresponded to the proton range was measured. Defects in silicon cause to increase the electric resistance by carrier compensation when proton dose is as high as $1*10^{13}$p/cm$^2$[14)]. Therefore, the depth profile of the resistance reflects the depth profile of the defects. Fig. 2-1 shows the depth profiles of the $R_{SR}$ in n-type silicon. They were measured before and after irradiation of protons with the energy of 4.5MeV up to the dose of $1*10^{13}$p/cm$^2$. In this

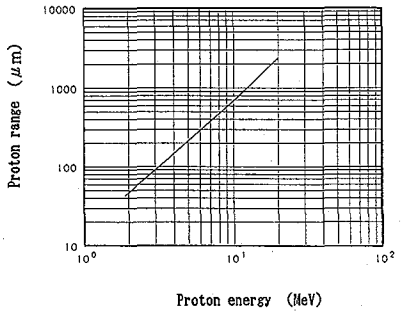


Fig. 1. The relationship between the proton range and the proton energy in silicon.

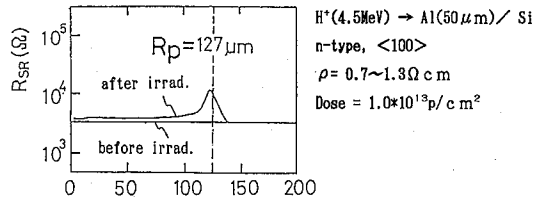


Fig.2-1.

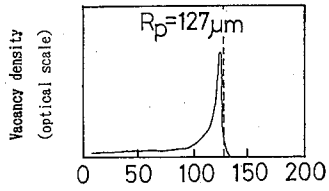


Fig.2-2.

Fig. 2–1. Spreading resistance profile in n–type silicon.
Fig. 2–2. Calculated defect (vacancy) profile

figure, the calculated range of the proton with the energy of 4.5MeV in silicon is also shown as the dashed line at the depth of 127$\mu$m. After the irradiation, the $R_{SR}$ increases around the end of the proton range and forms the peak at the left side of the range. Fig. 2–2 shows the density profile of defects (vacancies) by the simulation program "TRIM" for the same irradiation condition in fig. 2–1. Comparing both figures, the position of the peak in the $R_{SR}$ profile coincides with that for the peak in the calculated defect density profile. This fact indicates that the spreading resistance method is useful for monitoring the proton range.

There have been some reports about the new evaluation techniques for measuring directly the lifetime profile along the depth direction[15)16)17)]. However, it is difficult to measure the lifetime profile in the localized control area. In this experiment, the spreading resistance method was adopted.

Protons were injected perpendicular to the surface of the sample devices upon the cathode side or the anode side in the ambient pressure as low as $1*10^{-6}$Torr. After irradiation, irradiated sample devices were annealed at 350℃ for 2hrs in $N_2$ gas.

For the reference, we fabricated the thyristors whose lifetime was controlled by the gold diffusion. The gold atoms were diffused at 720℃ for 1hr in $N_2$ gas.

Measurements of the electrical characteristics were performed with the package of "the full pressure contact structure"[18)] at 125℃.

## EXPERIMENTAL RESULTS

Fig. 3 shows a schematic cross section of the diode and an illustration explaining how to irradiate the diode by proton beam with various energies. Protons were injected on cathode surface through an Al absorber with the thickness of 20$\mu$m at energies of 8.5, 6.3 and 3.5MeV. The Al absorber was used to hold the sample devices. It is well known that the reduction of the carrier lifetime in $N^-$ region is effective for reducing the reverse recovery charge which is

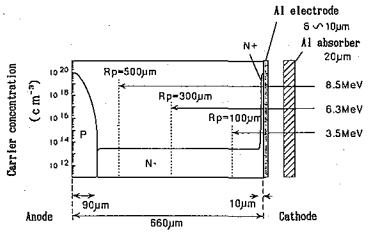


Fig. 3. Schematic cross section of the diode and an illustration explaining how to irradiate the diode by proton beam with various energies.

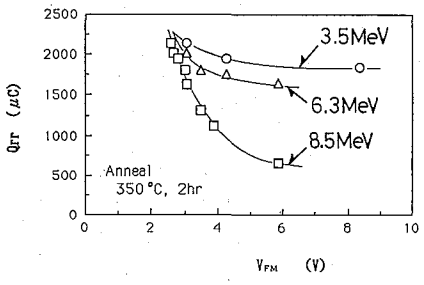


Fig. 4. The trade–off curves between the reverse recovery charge and the on–state voltage obtained for the diode.

proportional to the reverse recovery time. Fig. 4 shows the trade–off curves between the reverse recovery charge ($Q_{rr}$) and the on–state voltage ($V_{FM}$) obtained for the diode. The data points move toward the right direction along the curve as proton dose increases. The trade–off curve clearly varies with proton energy, which means the proton range. For getting the best trade–off curve, it is necessary to locate the proton range in the $N^-$ region near the $P/N^-$ junction. The similar result was previously obtained for the integral diode in shorted collector IGBT [19].

Fig. 5 shows the schematic cross section of the thyristor and an illustration explaining how to irradiate the thyristor by proton beam with various energies. Protons with four different energies were injected on anode surface through 20$\mu$m$^t$ Al absorber. Fig. 6 shows the trade–off curves between the reverse recovery charge ($Q_{rr}$) and the on–state voltage ($V_{TM}$) obtained for the thyristor. From this figure, it is clear that 4MeV proton irradiation gives the best trade–off curve. The location of the 4MeV proton range in thyristor is in the $N_B$ layer near the $P_E/N_B$ junction. This is same as that in diode. Fig. 7 shows the trade–off curves between the turn–off time and the on–state voltage ($V_{TM}$). It is clear that 7.5MeV proton irradiation gives the best trade–off curve. In this case, the location of the proton range is about middle of the $N_B$ layer. Thus the location of the proton range for the best trade–off curve between the reverse recovery charge and the on–state voltage apparently differs from that for the best trade–off curve between the turn–off time and the on–state voltage.

From fig. 6 and fig. 7, it is clear that the proton irradiation technology gives better trade–off curves than that by the gold diffusion. In these samples, no decline of blocking voltage by the proton irradiation was found.

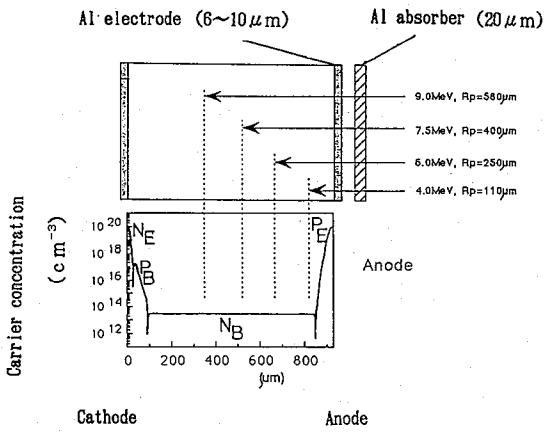


Fig. 5. Schematic cross section of the thyristor and an illustration explaining how to irradiate the thyristor by proton beam with various energies.

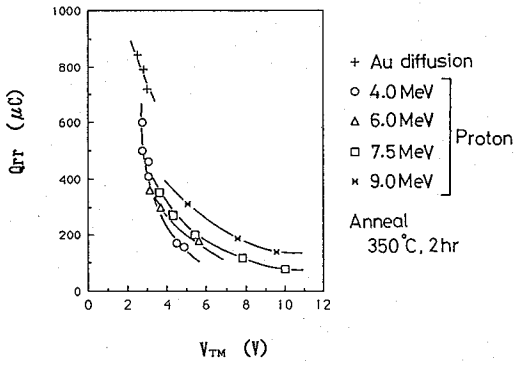


Fig. 6. The trade-off curves between the reverse recovery charge and the on-state voltage obtained for the thyristor. (Proton energy dependence)

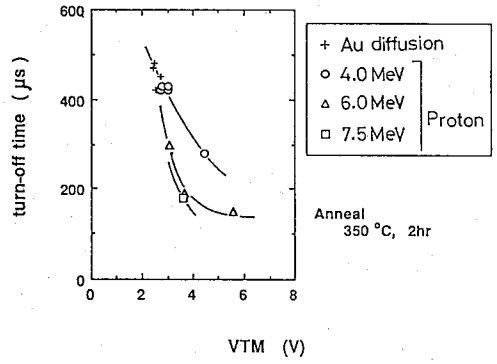


Fig. 7. The trade-off curves between the turn-off time and the on-state voltage obtained for the thyristor. (Proton energy dependence)

## CONCLUSION

We studied a lifetime control technology which localizes the presence of the carrier recombination centers in the depth of the devices by the proton irradiation. By this technology, we obtained the better trade-off curves between the turn-off time (include the reverse recovery charge) and the on-state voltage compared with the gold diffusion for the high power large size diode and thyristor. The trade-off curve varied with the position of the proton range. Moreover, it was found that the position of the proton range for the best trade-off relation corresponding to the reverse recovery charge differed from that corresponding to the turn-off time.

## ACKNOWLEDGMENTS

The authors would like to thank Prof. S. Kobayashi and Dr. M. Nakamura for their encouragement and assistance to use the accelerator. Mr. O. Kurakake is appreciated for his technical assistance of the electrical measurements.

## REFERENCES

1) B. J. Baliga and E. Sun, *IEEE Trans. Electron Devices*, vol. ED-24, pp. 685-688 (1977).
2) B. J. Baliga "Silicon power field controlled devices and integrated circuits," in Silicon Integrated Circuits, D. Kahng, Ed., Applied Solid State Science Series, supp. 2B. New York : Academic, pp. 110-274 (1981).
3) A. M. Campero, R. P. Love, M. F. Chang and R. F. Dyer, *IEEE Trans. Electron Devices*, vol. ED-33, No. 11 (1986).
4) A. M. Campero, R. P. Love, M. F. Chang and R. F. Dyer, *Solid-State Electronics*, vol. 30, No. 2, pp. 185-188 (1987).
5) H. Akiyama, M. Harada, H. Kondoh and Y. Akasaka, *Proc. of ISPSD '91*, pp. 187-191 (1991).
6) W. Wondrak, W. -D. Nowak and B. Thomas, *Proc. of ISPSD '88*, pp. 147-152 (1988).
7) A. Hallén and M. Bakowski, *Solid-State Electronics*, vol. 32, No. 11, pp. 1033-1037 (1989).
8) Y. Shimizu, T. Yokota and I. Kohno, *Proc. of ISPSD '90*, pp. 231-235 (1990).
9) M. Nakamura, S. Shimomura, K. Takimoto, H. Sakaguchi and S. Kobayashi, *Nuclear Instruments and Methods in Physics Research*, **A268**, pp. 313-315 (1988).
10) A. Hallén, P. A. Ingemarsson, P. HÅkansson, B. U. R. Snudqvist and G. Possnert, *Nuclear Instruments and Methods in Physics Research*, **B36**, pp. 345-349 (1989).
11) K. L. Brown, F. Rothacker, D. C. Carey and Ch. Iselin, CERN 80-04, Super Proton Synchrotron Division, 18 March (1980).
12) K. Matsuda and S. Nagai, JAERI-M 8471 (1979).
13) H. Sunaga, T. Agematsu, R. Tanaka, K. Yoshida and I. Kohno, *RIKEN Accel. Prog. Rep.*, 21 (1987).
14) A. Mogro-Camperc, M. F. Chang and J. L. Benjamin, *J. Electrochem. Soc.*, vol. 135, No. 1, pp. 172-176 (1988).
15) T. Flohr and R. Helbig, *IEEE Trans. Electron Devices*, vol. 37, No. 9 (1990).
16) A. Hallén, B. U. R. Sundqvist, Z. Paska, B. G. Svensson, M. Rosling and J. Tirén, *J. Appl. Phys.*, **67**(3), 1 Feb. (1990).
17) M. Rosling, H. Bleichner and E. Nordlander, *Proc. of EPE-MADEP '91*, pp. 59-64 (1991).
18) H. Iwamoto, T. Nakagawa, F. Tokunoh, A. Tada, Y. Yamauchi, M. Yamamoto and K. Satoh, *Proc. of ISPSD '90*, pp. 283-288 (1990).
19) H. Akiyama, M. Harada, H. Kondoh, Y. Akasaka, (in Japanese) *National Convention Record I. E.E. Japan*, **463**, pp. 5-22 (1991).